

# Compact finite difference scheme for option pricing in Heston's model

Bertram Düring\* and Michel Fournié†

\**Institut für Analysis und Scientific Computing, Technische Universität Wien,  
Wiedner Hauptstraße 8–10, 1040 Wien, Austria.*

†*Institut de Mathématiques de Toulouse, Equipe 'Mathématiques pour l'Industrie et la Physique',  
CNRS, Unité Mixte 5219, Université Paul Sabatier, 118, route de Narbonne, 31062 Toulouse cedex, France.*

**Abstract.** We present a compact high-order finite difference scheme for option pricing in the well-known Heston stochastic volatility model. The scheme is fourth order accurate in space and second order accurate in time. This is also confirmed by the numerical experiments that we present.

**Keywords:** Option pricing, compact finite difference discretizations, stochastic volatility.  
**PACS:** 02.60.Lj, 02.70.Bf, 89.65.Gh

## INTRODUCTION

One widely used stochastic volatility model for option pricing is Heston's model [6]. It is based on a two-dimensional stochastic diffusion process with two correlated Brownian motions. Let  $W = (W^{(1)}, W^{(2)})$  denote a two-dimensional Brownian motion with correlation  $dW^{(1)}(t)dW^{(2)}(t) = \rho dt$  on a given filtered probability space. The value of the underlying asset in [6] follows

$$dS(t) = \bar{\mu}S(t)dt + \sqrt{\sigma(t)}S(t)dW^{(1)}(t), \quad d\sigma(t) = \kappa^*(\theta^* - \sigma(t))dt + v\sqrt{\sigma(t)}dW^{(2)}(t), \quad (1)$$

for  $0 < t \leq T$  with  $S(0), \sigma(0) > 0$  where  $\bar{\mu}$ ,  $\kappa^*$ ,  $v$  and  $\theta^*$  denote the drift, the mean reversion speed, the volatility of volatility and the long-run mean of  $\sigma$ , respectively. Heston [6] shows that the option price  $V = V(S, \sigma, t)$  solves the following partial differential equation

$$V_t + \frac{1}{2}S^2\sigma V_{SS} + \rho v\sigma S V_{S\sigma} + \frac{1}{2}v^2\sigma V_{\sigma\sigma} + rSV_S + [\kappa^*(\theta^* - \sigma) - \lambda\sigma]V_\sigma - rV = 0, \quad (2)$$

for  $S, \sigma > 0$ ,  $0 \leq t < T$  and subject to a suitable final condition, e.g.,  $V(S, \sigma, T) = \max(K - S, 0)$ , in case of a European put option with strike price  $K$ . In (2),  $\lambda$  is a constant parameter for the market price of volatility risk. As it is common in the literature we introduce the modified parameters,  $\kappa = \kappa^* + \lambda$ ,  $\theta = \kappa^*\theta^*/(\kappa^* + \lambda)$ , which allow us to study the problem with one parameter less. The 'boundary' conditions in the case of the put option read as follows

$$\begin{aligned} V(0, \sigma, t) &= Ke^{-r(T-t)}, & T > t \geq 0, \sigma > 0, & & V(S, \sigma, t) \rightarrow 0, & T > t \geq 0, \sigma > 0, \text{ as } S \rightarrow \infty, \\ V_\sigma(S, \sigma, t) &\rightarrow 0, & T > t \geq 0, S > 0, \text{ as } \sigma \rightarrow \infty, & & V_\sigma(S, \sigma, t) \rightarrow 0, & T > t \geq 0, S > 0, \text{ as } \sigma \rightarrow 0. \end{aligned}$$

For *constant* parameters, one can employ Fourier transform techniques and obtain a system of ordinary differential equations which can be solved analytically [6]. In general, however, when the coefficients are not constant, equation (2) has to be solved numerically. Another approach is to derive approximate analytic expressions, see, e.g., [1] and the literature cited therein.

In the mathematical literature, there are many papers on numerical methods for option pricing, mostly addressing the case of a single risk factor and using standard, second order finite difference methods (see, e.g., [13] and the references therein). More recently, higher-order finite difference schemes (fourth-order in space) were proposed that use a compact stencil (three points in space). In the present context see, e.g., [12] for linear and [4, 5, 10] for fully nonlinear problems. There are less works considering numerical methods for option pricing in stochastic volatility models, i.e., for two spatial dimensions. Finite difference approaches that are used are often standard, low order

methods (second order in space) and little numerical analysis or convergence results are provided. Other approaches include finite element-finite volume [15], multigrid [2], sparse wavelet [9], and spectral methods [14].

Let us review some of the related finite difference literature. Different efficient methods for solving the American option pricing problem for the Heston model are compared in [8]. The article focusses on the treatment of the early exercise free boundary and uses a second order finite difference discretization. In [7] different, low order ADI (alternating direction implicit) schemes are adapted to the Heston model to include the mixed spatial derivative term. While most of [12] focusses on a compact high-order scheme for the standard (one-dimensional) case, in a short remark [12, Section 5] also the stochastic volatility (two-dimensional) case is considered. However, the final scheme there is of second order only due to the low order approximation of the cross diffusion term.

In this work we consider a *compact finite difference scheme* for (two-dimensional) option pricing in the Heston model. This compact scheme has been derived in [3]. It is fourth order accurate in space and second order accurate in time. Results on the unconditional stability in the sense of von Neumann and convergence of the scheme are given in [3]. We present numerical experiments that confirm the good properties of the method.

## HIGH ORDER COMPACT SCHEME

### Transformation of the equation

Under the transformation of variables  $x = \ln(S/K)$ ,  $y = \sigma/v$ ,  $\tilde{t} = T - t$ ,  $u = \exp(r\tilde{t})V/K$ , (we immediately drop the tilde in the following) and using the modified parameters,  $\kappa$  and  $\theta$ , we obtain from (2),

$$u_t - \frac{1}{2}vy(u_{xx} + u_{yy}) - \rho vy u_{xy} + \left(\frac{1}{2}vy - r\right)u_x - \kappa \frac{\theta - vy}{v}u_y = 0, \quad (3)$$

to be solved on  $\mathbb{R} \times \mathbb{R}^+$  with the following initial and boundary conditions:

$$\begin{aligned} u(x, \sigma, 0) &= \max(1 - \exp(x), 0), & x \in \mathbb{R}, \sigma > 0, \\ u(x, \sigma, t) &\rightarrow 1, & x \rightarrow -\infty, \sigma > 0, t > 0, \\ u_\sigma(x, \sigma, t) &\rightarrow 0, & x \in \mathbb{R}, \sigma \rightarrow \infty, t > 0, \\ u(x, \sigma, t) &\rightarrow 0, & x \rightarrow +\infty, \sigma > 0, t > 0, \\ u_\sigma(x, \sigma, t) &\rightarrow 0, & x \in \mathbb{R}, \sigma \rightarrow 0, t > 0. \end{aligned}$$

### Definition of the scheme

For the discretization, we replace  $\mathbb{R}$  by  $[-R_1, R_1]$  and  $\mathbb{R}^+$  by  $[0, R_2]$  with  $R_1, R_2 > 0$ . For simplicity, we consider a uniform grid with mesh width  $h$  in both the  $x$ - and  $y$ -direction,  $Z = \{x_i \in [-R_1, R_1] : x_i = ih, i = -N, \dots, N\} \times \{y_j \in [0, R_2] : y_j = jh, j = 0, \dots, M\}$  consisting of  $(2N + 1) \times (M + 1)$  grid points, with  $R_1 = Nh$ ,  $R_2 = Mh$  and time step  $k$ . Let  $u_{ij}^n$  denote the approximate solution of (3) in  $(x_i, y_j)$  at the time  $t_n = nk$  and let  $u^n = (u_{ij}^n)$ . On the truncated numerical domain we impose artificial boundary conditions. We impose Dirichlet conditions on two boundaries, i.e.,  $u_{-Nj}^n = 1$ ,  $u_{+Nj}^n = 0$ , ( $j = 0, \dots, M$ ), while we use homogeneous Neumann conditions at the other boundaries.

The fourth-order compact finite difference scheme derived in [3] uses a nine-point computational stencil involving the eight nearest neighboring points of the reference grid point  $(i, j)$ . Associated to the shape of the computational stencil, we introduce indexes for each node from 0 to 9,

$$\begin{pmatrix} u_{i-1, j+1} = u_6 & u_{i, j+1} = u_2 & u_{i+1, j+1} = u_5 \\ u_{i-1, j} = u_3 & u_{i, j} = u_0 & u_{i+1, j} = u_1 \\ u_{i-1, j-1} = u_7 & u_{i, j-1} = u_4 & u_{i+1, j-1} = u_8 \end{pmatrix}.$$

The idea behind the derivation of the high-order compact scheme is to operate on the differential equation as an additional relation to obtain finite difference approximations for high-order derivatives in the truncation error. Inclusion of these expressions in a central difference method for equation (3) increases the order of accuracy to  $\mathcal{O}(h^4)$  while retaining a compact stencil. Different time integrators can be implemented. We consider the most common class of methods involving two times steps, differencing at time  $t_\mu = (1 - \mu)t^n + \mu t^{n+1}$ , where  $0 \leq \mu \leq 1$  and the superscript  $n$  denotes the time level. This yields a class of integrators that include the forward Euler ( $\mu = 0$ ), Crank-Nicolson ( $\mu = 1/2$ ) and backward Euler ( $\mu = 1$ ) schemes. Details of the derivation and a thorough Fourier analysis for the von Neumann stability are presented in [3].

The resulting fully discrete difference scheme for node  $(i, j)$  at the time level  $n$  can be written in the form

$$\sum_{l=0}^8 \beta_l u_i^{n+1} = \sum_{l=0}^8 \zeta_l u_i^n, \quad (4)$$

where the coefficients  $\beta_l, \zeta_l$  are given by

$$\begin{aligned} \beta_0 &= (((2y_j^2 - 8)v^4 + ((-8\kappa - 8r)y_j - 8\rho r)v^3 + (8\kappa^2 y_j^2 + 8r^2)v^2, -16\kappa^2 \theta v y_j + 8\kappa^2 \theta^2) \mu k + 16v^3 y_j) h^2 \\ &\quad + (-16\rho^2 + 40)y_j^2 v^4 \mu k, \\ \beta_{1,3} &= \pm ((\kappa \theta v^2 - v^4 - \kappa y_j v^3) \mu k - (y_j + 2\rho)v^3 + 2v^2 r) h^3 + (((-y_j^2 + 2)v^4 + ((4r + 2\kappa)y_j + 4\rho r)v^3 \\ &\quad - (2\kappa \theta + 4r^2)v^2) \mu k + 2v^3 y_j) h^2 \pm (4v^4 y_j^2 + (-8y_j^2 \kappa \rho - 8y_j r)v^3 + 8y_j \kappa \theta \rho v^2) \mu k h + (8\rho^2 - 8)y_j^2 v^4 \mu k, \\ \beta_{2,4} &= \pm ((2\kappa^2 \theta v - 2\kappa^2 v^2 y_j - 2v^3 \kappa) \mu k - 2v^2 y_j \kappa + 2v \kappa \theta - 2v^3) h^3 + ((2v^4 + 2\kappa y_j v^3 + (-4\kappa^2 y_j^2 + 2\kappa \theta)v^2 \\ &\quad + 8\kappa^2 \theta v y_j - 4\kappa^2 \theta^2) \mu k + 2v^3 y_j) h^2 \pm ((8y_j^2 \kappa + 8y_j \rho r)v^3 - 4v^4 y_j^2 \rho - 8v^2 y_j \kappa \theta) \mu k h + (8\rho^2 - 8)y_j^2 v^4 \mu k, \\ \beta_{5,7} &= ((v^4 \rho + (-y^2 \kappa + \kappa y_j \rho + r)v^3 + (\theta + 2r) \kappa y_j v^2 - 2r \kappa \theta v) \mu k + v^3 \rho y_j) h^2 \pm ((2\rho + 1)y_j^2 v^4 + ((2 + 4\rho) \kappa y_j^2 \\ &\quad + (-4\rho r - 2r)y_j)v^3 + (-2\theta - 4\theta \rho) \kappa y_j v^2) \mu k h + (-2 - 4\rho^2 - 6\rho)y_j^2 v^4 \mu k, \\ \beta_{6,8} &= ((-v^4 \rho + (y_j^2 \kappa - \kappa y_j \rho - r)v^3 + (-\theta - 2r) \kappa y_j v^2 + 2r \kappa \theta v) \mu k - v^3 \rho y_j) h^2 \pm ((2\rho - 1)y_j^2 v^4 + ((2 - 4\rho) \kappa y_j^2 \\ &\quad + (2r - 4\rho r)y_j)v^3 + (4\theta \rho - 2\theta) \kappa y_j v^2) \mu k h + (-4\rho^2 + 6\rho - 2)y_j^2 v^4 \mu k, \end{aligned}$$

and

$$\begin{aligned} \zeta_0 &= 16v^3 y_j h^2 + (1 - \mu) k (((8 - 2y_j^2)v^4 + ((8\kappa + 8r)y_j + 8\rho r)v^3 + (-8r^2 - 8\kappa^2 y_j^2)v^2 + 16\kappa^2 \theta v y_j - 8\kappa^2 \theta^2) h^2 \\ &\quad + (-40 + 16\rho^2) y_j^2 v^4), \\ \zeta_{1,3} &= \pm (2r - (y_j + 2\rho)v) v^2 h^3 + 2v^3 y_j h^2 + (1 - \mu) k (\pm (v \kappa y_j + v^2 - \kappa \theta) v^2 h^3 + (v^2 y_j^2 - (4r + 2\kappa) v y_j + 4r^2 + 2\kappa \theta \\ &\quad - 2v^2 - 4\rho v r) v^2 h^2 \pm ((-4v + 8\kappa \rho) v^3 y_j^2 + (-8\kappa \theta \rho + 8vr) v^2 y_j) h + (8v^2 - 8v^2 \rho^2) v^2 y_j^2), \\ \zeta_{2,4} &= \pm (2v \kappa \theta - 2v^2 y_j \kappa - 2v^3) h^3 + 2v^3 y_j h^2 + (1 - \mu) k (\pm 2(v^2 - \kappa \theta + \kappa v y_j) \kappa v h^3 + (4\kappa^2 v^2 y_j^2 - (2v^2 + 8\kappa \theta) \kappa v y_j \\ &\quad + 2\kappa \theta (2\kappa \theta - v^2) - 2v^4) h^2 \pm ((-8v^3 \kappa + 4v^4 \rho) y_j^2 + (8\kappa \theta v^2 - 8v^3 \rho r) y_j) h + (-8v^4 \rho^2 + 8v^4) y_j^2), \\ \zeta_{5,7} &= v^3 \rho y_j h^2 + (1 - \mu) k ((v^3 y_j^2 \kappa - v(v \kappa \theta + 2r \kappa v + \kappa v^2 \rho) y_j - v(v^2 r - 2r \kappa \theta + v^3 \rho)) h^2 \\ &\quad \pm (-v(2v^3 \rho + v^3 + 4\kappa v^2 \rho + 2v^2 \kappa) y_j^2 + v(2v \kappa \theta + 4v \kappa \theta \rho + 4v^2 \rho r + 2v^2 r) y_j) h + v(2v^3 + 6v^3 \rho + 4v^3 \rho^2) y_j^2), \\ \zeta_{6,8} &= -v^3 \rho y_j h^2 + (1 - \mu) k ((-v^3 y_j^2 \kappa + v(v \kappa \theta + 2r \kappa v + \kappa v^2 \rho) y_j + v(v^2 r - 2r \kappa \theta + v^3 \rho)) h^2 \\ &\quad \pm (v(-2v^3 \rho + v^3 + 4\kappa v^2 \rho - 2v^2 \kappa) y_j^2 + v(2v \kappa \theta - 4v \kappa \theta \rho + 4v^2 \rho r - 2v^2 r) y_j) h + v(2v^3 - 6v^3 \rho + 4v^3 \rho^2) y_j^2). \end{aligned}$$

When multiple indexes are used with  $\pm$  and  $\mp$  signs, the first and second index corresponds to the upper and lower sign, respectively. Choosing  $\mu = 1/2$ , i.e., in the Crank-Nicolson case, the resulting scheme is of order two in time and order four in space.

## NUMERICAL RESULTS

In this section we perform a numerical study to compute the order of convergence of the scheme. Due to the compact discretization of (4) the resulting linear systems have a good sparsity pattern and can be solved very efficiently. We use the parameters  $K = 100$ ,  $T = 0.5$ ,  $r = 0.05$ ,  $v = 0.1$ ,  $\kappa = 2$ ,  $\theta = 0.01$ ,  $\rho = -0.5$ . For the parameter  $\mu$  we use a Rannacher time-stepping choice [11], i.e., we start with four fully implicit quarter time steps ( $\mu = 1$ ) and then continue with Crank-Nicolson ( $\mu = 1/2$ ). We fix the parabolic mesh ratio  $k/h^2$  to a constant value.

We compute the  $l_2$  norm error  $\varepsilon_2$  and the maximum norm error  $\varepsilon_\infty$  of the numerical solution. Then, asymptotically, we expect these errors to converge as  $\varepsilon = Ch^m$  for some  $m$  and  $C$  representing a constant. This implies  $\ln(\varepsilon) = \ln(C) + m \ln(h)$ . Hence, the double-logarithmic plot  $\varepsilon$  against  $h$  should be asymptotic to a straight line with slope  $m$ . This gives a method for experimentally determining the order of the scheme.

We refer to Figure 1 for the results using the parameters given above. For comparison we conducted additional experiments using a standard, second order scheme. We observe that the numerical convergence order agrees well with the theoretical order of the schemes for carefully smoothed initial condition. For non-smooth initial condition the numerical convergence order of the high order compact scheme is reduced to about two. The error in the maximum norm in this case, however, is still smaller by a factor 1.5 – 2 than the error for the standard scheme for comparable numerical effort.

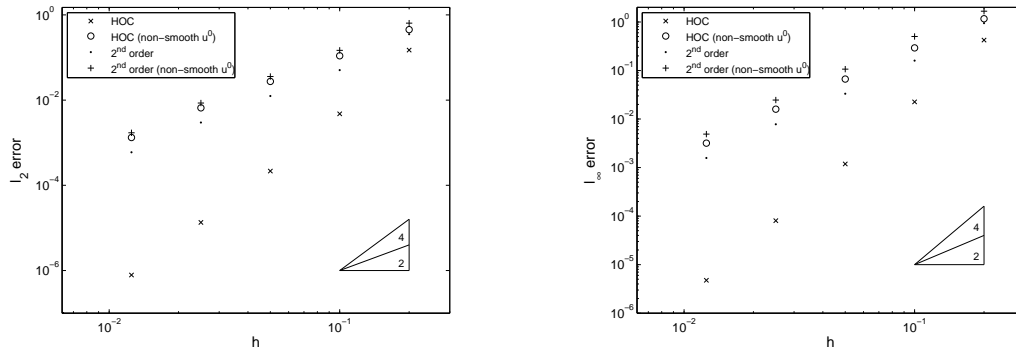


FIGURE 1.  $l_2$ -error vs.  $h$  (left) and  $l_\infty$ -error vs.  $h$  (right).

## ACKNOWLEDGMENTS

Bertram Düring acknowledges support from the Austrian Science Fund (FWF), grant P20214, and from the Austrian-Croatian Project HR 01/2010 of the Austrian Exchange Service (ÖAD).

## REFERENCES

1. E. Benhamou, E. Gobet, and M. Miri. Time Dependent Heston Model, *SIAM J. Finan. Math.* **1**, 289–325, 2010.
2. N. Clarke and K. Parrott. Multigrid for American option pricing with stochastic volatility. *Appl. Math. Finance* **6**(3), 177–195, 1999.
3. B. Düring and M. Fournié. High-order compact finite difference scheme for option pricing in stochastic volatility models, preprint, 2010.
4. B. Düring, M. Fournié, and A. Jüngel. Convergence of a high-order compact finite difference scheme for a nonlinear Black-Scholes equation. *Math. Mod. Num. Anal.* **38**(2), 359–369, 2004.
5. B. Düring, M. Fournié, and A. Jüngel. High-order compact finite difference schemes for a nonlinear Black-Scholes equation. *Intern. J. Theor. Appl. Finance* **6**(7), 767–789, 2003.
6. S.L. Heston. A closed-form solution for options with stochastic volatility with applications to bond and currency options. *Review of Financial Studies* **6**(2), 327–343, 1993.
7. K.J. in't Hout and S. Foulon. ADI finite difference schemes for option pricing in the Heston model with correlation, *Int. J. Numer. Anal. Mod.* **7**, 303–320, 2010.
8. S. Ikonen and J. Toivanen. Efficient numerical methods for pricing American options under stochastic volatility, *Numer. Methods Partial Differential Equations* **24**(1), 104–126, 2008.
9. N. Hilber, A. Matache, and C. Schwab. Sparse wavelet methods for option pricing under stochastic volatility. *J. Comput. Financ.* **8**(4), 1–42, 2005.
10. W. Liao and A.Q.M. Khaliq. High-order compact scheme for solving nonlinear Black-Scholes equation with transaction cost, *Int. J. Comput. Math.* **86**(6), 1009–1023, 2009.
11. R. Rannacher. Finite element solution of diffusion problems with irregular data, *Numer. Math.* **43**(2), 309–327, 1984.
12. D.Y. Tangman, A. Gopaul, and M. Bhuruth. Numerical pricing of options using high-order compact finite difference schemes. *J. Comp. Appl. Math.* **218**(2), 270–280, 2008.
13. D. Tavella and C. Randall. *Pricing Financial Instruments: The Finite Difference Method*. John Wiley & Sons, 2000.
14. W. Zhu and D.A. Kopriva. A spectral element approximation to price European options with one asset and stochastic volatility. *J. Sci. Comput.* **42**(3), 426–446, 2010.
15. R. Zvan, P.A. Forsyth, and K.R. Vetzal. Penalty methods for American options with stochastic volatility. *J. Comp. Appl. Math.* **91**(2), 199–218, 1998.